

ESR STUDIES OF POLYMERS IN THE BULK PHASE

G. Gordon Cameron

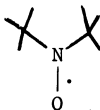
Department of Chemistry, University of Aberdeen, Aberdeen, Scotland

Abstract - The scope and limitations of the spin-probe and spin-label techniques for studying polymers in the bulk state are reviewed. Methods of calculating correlation times for rotational diffusion of nitroxides from their ESR spectra are described. The significance of the T_{50G} parameter is discussed with particular reference to spin-probed poly(vinyl acetate). The spin-label technique is illustrated by reference to polyethylene in the solid and molten states, and in solution.

INTRODUCTION

The spin-label and spin-probe techniques were applied first to studies of biological macromolecules (Ref. 1) and four or five years elapsed before applications to synthetic polymers were reported. In the spin-label experiment a stable free radical is bound by a covalent bond to the polymer chain, and in the spin-probe experiment the radicals are simply dispersed in the polymer matrix and interactions with polymer chains are through secondary valence forces. The frequency of radical tumbling can be determined from the spectrum of the labelled or probed polymer and this in turn can yield information on the dynamics and relaxations of the polymer. These ESR methods provide information in the frequency range $10^2 - 10^{10}$ Hz and therefore complement other techniques such as mechanical, NMR, dielectric and ultrasonic relaxation which cover other frequency ranges.

Of the available stable radicals that might function as probes or labels in polymers only nitroxide (nitroxyl) radicals have been used successfully. The reasons for this are: (i) nitroxides are often remarkably stable (label and probe experiments have been conducted at 440K), (ii) nitroxides of widely varying structures, some with functional groups to facilitate labelling, can be synthesised, and (iii) nitroxides have well-defined g -tensors and hyperfine coupling tensors to the ^{14}N nucleus. The last property is a fundamental requirement for obtaining quantitative dynamic data from an analysis of an ESR spectrum. Most of the useful nitroxide radicals are of the di-*t*-alkyl type



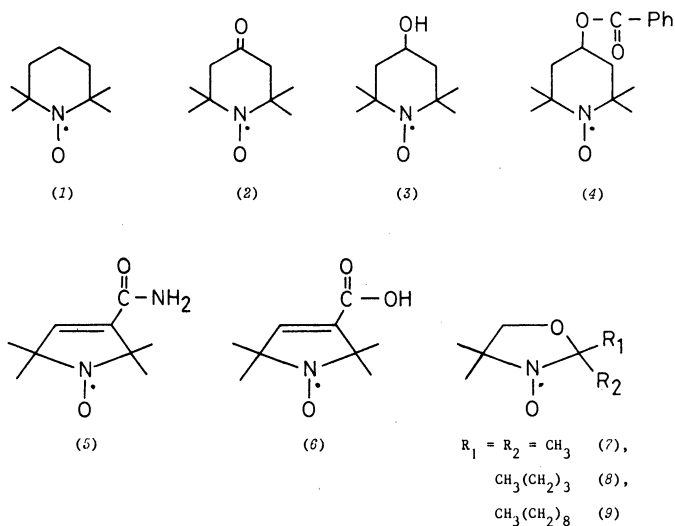
in which the bulky side groups hinder decomposition reactions.

Because the ESR method is highly sensitive very low radical concentrations are employed (down to 10^{-6} M in some cases) and line broadening effects due to spin exchange are easily avoided.

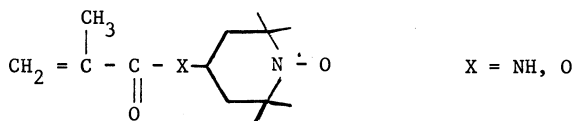
The correlation times for nitroxide radical tumbling fall into three time regimes: (i) fast $10^{-11} - 10^{-9}$ s, (ii) slow $10^{-9} - 10^{-7}$ s, and (iii) very slow $10^{-7} - 10^{-3}$ s. The limits to these regions are determined by the anisotropies of the magnetic interactions that occur in nitroxide radicals. In this article we are concerned with regions (i) and (ii) which yield quite distinct and characteristic ESR spectra. In bulk polymers correlation times of nitroxide probes and labels are mostly in the slow region.

Di-*t*-alkyl substituted piperidine and pyrroline derivatives are commonly used as spin probes. Representative examples of these and other nitroxide probes are shown in Table 1. Several nitroxide spin probes and labels are now available commercially.

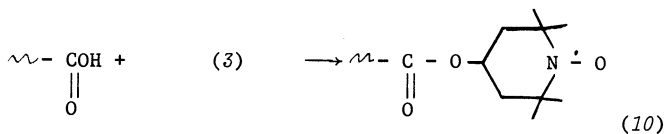
TABLE 1. Examples of nitroxide spin probes



The spin-label experiment requires the nitroxide moiety to be covalently bonded to the polymer, preferably at a known position. Attempts to incorporate labelled units directly by copolymerisation with nitroxide-carrying monomer such as



have not been very successful because the propagating radical or ion reacts readily with the nitroxide group, so that low polymers are generally produced. If a nitroxide with a functional group able to condense with an appropriate group on the subject polymers is available, then labelling may be quite straightforward. For example, the hydroxyl group on spin probe (3) may be esterified with a carboxyl or acid chloride group on a polymer



There are many obvious variants on this type of reaction.

If direct attachment of a preformed nitroxide to the polymer is not possible, then an indirect synthesis may have to be adopted. Two examples of such syntheses are shown below

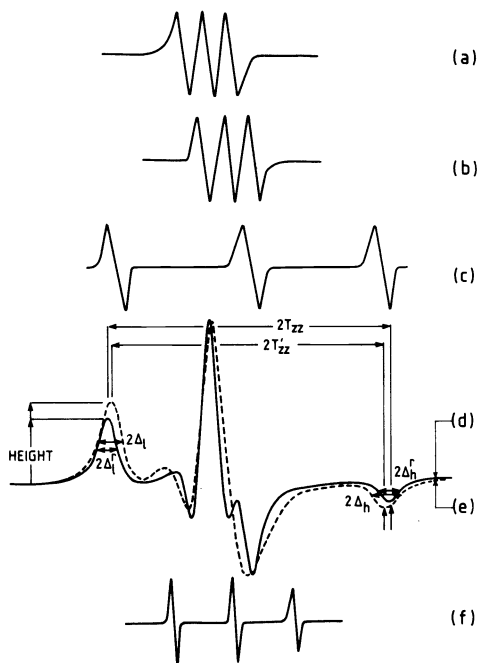


Fig. 2. Idealised ESR spectra of nitroxide radicals: (a), (b) and (c) are single crystal spectra with the applied magnetic field along the x, y and z principal axes respectively of the g- and T-tensors. (d) is a rigid limit powder spectrum and (e) is a powder spectrum for nitroxide radicals in the slow tumbling region. (f) is a solution spectrum in the rapidly tumbling region. (Spectra in (d) and (e) taken with permission from Ref. 8).

where T_{xx} , T_{yy} and T_{zz} are the principal values of the coupling tensor. From eqn. 1 $\tau_c \approx 3 \times 10^{-9}$ s. When τ_c is $< 3 \times 10^{-9}$ s the radicals are undergoing sufficiently rapid rotational diffusion to average out the anisotropies of the g- and coupling tensors. The resulting spectrum is of the "motionally-narrowed" form shown in Fig. 2f, which is typical of nitroxide molecules in dilute solution with correlation times in the fast range (i). The spectra in Fig. 2d and 2e are strikingly different from Fig. 2f. The lines in the latter are narrower and sharper and the outermost lines are separated typically by 35-40G compared with 60-65G for the slow-motion spectra.

The changes in the ESR spectrum that occur when a nitroxide radical increases in tumbling frequency through the slow region may be used to calculate rotational correlation times. This is possible because several theoretical approaches have been developed to simulate the ESR spectra of nitroxide radicals in the slow-motion region (Refs. 6, 7, 8). Thus, Fig. 3 shows how the inward shifts of the high- and low-field extrema depend on correlation time. This method is most useful for calculating correlation times in the range 10^{-8} s $< \tau_c < 10^{-7}$ s, and the high-field line is believed to be the more useful because it undergoes a greater shift, remains separate from central spectral features for shorter values of τ_c , and is insensitive to small variations in the principal values of \hat{T} and \hat{g} .

The inward shifts of the extrema are also used in the method of Goldman et al. (7) who defined a parameter $S = T'_{zz}/T_{zz}$, where T'_{zz} is one-half the separation of the extrema and $2T_{zz}$ is the rigid limit separation (see Fig. 2). The correlation time is related to S by

$$\tau_c = a(1-S)^d \quad (2)$$

Sets of values of a and d, which are both sensitive to the diffusion model chosen and to the residual line width, have been published (Ref. 7). The shortest correlation time obtainable by this method is ca. 7×10^{-9} s, because below this the outer lines converge rapidly to the motionally narrowed spectrum. The upper limit is set by the experimental precision with which S can be measured. Values of S greater than 0.99 cannot be measured accurately and for a residual line width of 0.3G and Brownian diffusion this corresponds to a correlation time of 9×10^{-7} s. For larger residual widths and other rotational models the situation is rather worse. The choice of diffusion model may be facilitated by determining the ratio of the high- to low-field extrema shifts, $\Delta H_h/\Delta H_l$. This ratio changes over a wider range for a Brownian than for a jump diffusion model (Ref. 9).

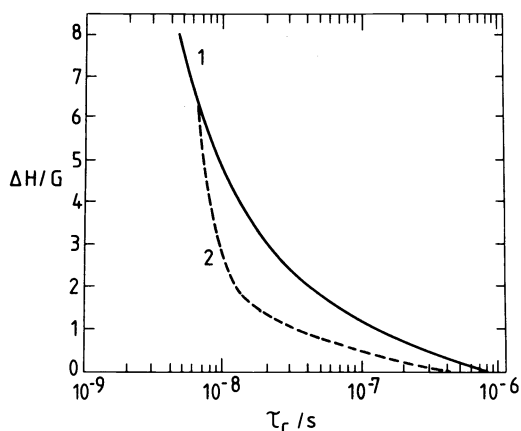


Fig. 3. Inward shifts ΔH of (1) high-field and (2) low-field extrema of the first derivative nitroxide spectrum as a function of τ_c . Brownian diffusion and axial symmetry of the g - and T -tensors is assumed. (Reproduced with permission from Ref. 6).

The life-time broadening effect, which is manifest by an initial increase in linewidth with the onset of motion (see Fig. 2d and 2e), has been related to τ_c by

$$\tau_c = a' (W_i - 1)^{-d'} \quad (3)$$

where the parameters a' and d' depend upon the diffusion model and the residual linewidth (Ref. 8). The parameter W_i is given by the ratio of the half-widths at half-height of the extrema

$$W_i = \Delta_i / \Delta_i^r \quad (4)$$

where $i = l, h$ (low- and high-field respectively) and the superscript r indicates the rigid limit value. The widths of the extrema are sensitive to relaxations in the microsecond region and by this method correlation times to $\tau_c < 5 \times 10^{-6}$ s may be measured.

When the motion of the radical or probe is markedly anisotropic the above methods are not reliable and recourse must be made to detailed spectral simulations for which computer programmes are now available (Ref. 10).

Correlation times of nitroxides tumbling in the fast regime 10^{-11} to 10^{-9} s where the spectra are of the motionally narrowed type in Fig. 2f, may be calculated from the linewidths. If the peak-to-peak width of the first derivative of a Lorentzian line is $\Delta\nu$ (Hz), then the linewidth parameter $T_2 = (\pi\sqrt{3} \Delta\nu)^{-1}$. In general, the dependence of T_2 upon m , the component of the nuclear spin along the direction of the applied magnetic field, is given by

$$T_2^{-1} (m) = A + Bm + Cm^2 \quad (5)$$

which shows that the three lines (corresponding to $m = 0, \pm 1$) are unequal in width (Ref. 11). For the particular case of isotropic rotational diffusion coupled with near-axial symmetry of the coupling tensor \hat{T} ($T_{xx} \approx T_{yy}$) the coefficients are:

$$A = \left[\frac{b^2}{20} (3 + 7u) + \frac{1}{15} (\Delta\gamma H_0)^2 \left(\frac{4}{3} + u \right) \right] \tau_c + \delta \quad (6a)$$

$$B = \frac{1}{5} b \Delta\gamma H_0 \left(\frac{4}{3} + u \right) \tau_c \quad (6b)$$

$$C = \frac{1}{8} b^2 \left(1 - \frac{u}{5} \right) \tau_c \quad (6c)$$

The parameters in Eq. 6a, b and c are defined as follows

$$b = (4\pi/3) [T_{zz} - \frac{1}{2}(T_{xx} + T_{yy})]$$

$$\Delta\gamma = \frac{|\beta|}{h} [g_{zz} - \frac{1}{2}(g_{xx} + g_{yy})]$$

$$u = (1 + \omega_0^2 \tau_c^2)^{-1}$$

where the principal values of \hat{T} are in Hz. H_0 and ω_0 are the applied magnetic field and the corresponding Larmor angular frequency respectively, while τ_c is the rotational correlation time. For isotropic Brownian diffusion $\tau_c = (6R)^{-1}$ where R is the rotational diffusion coefficient. For spin-labelling studies at X-band ($\omega_0 \approx 2\pi \times 9.3 \times 10^9$ rad s $^{-1}$) it is usually a good approximation to set u , the non-secular contribution to the linewidths, to zero. The coefficient A contains the term δ which represents contributions from mechanisms independent of m (e.g. spin exchange). However, the three equations implicit in eqn. 6 are readily rearranged to eliminate A and hence δ :

$$T_2(0)/T_2(m) = 1 + B T_2(0) m + C T_2(0) m^2 \quad (7)$$

If r_{\pm} is used to represent $T_2(0)/T_2(\pm 1)$ then two values of τ_c may be obtained from

$$r_+ + r_- - 2 = 2 C T_2(0) \quad (8a)$$

and

$$r_+ - r_- = 2 B T_2(0) \quad (8b)$$

In the case of the two values of τ_c not agreeing, the assumption of isotropic rotation must be suspected.

THE GLASS TRANSITION AND T_{50G}

At the critical value of τ_c defined by eqn. 1 the separation of the outermost lines ($2T'_{zz}$) in the ESR spectrum of a nitroxide is approximately 50G. In this condition the rate of nitroxide tumbling is midway between the fast and slow regions (i) and (ii). Many spin-probed polymers undergo this transition over a very narrow temperature range which may be characterised by the widely-used empirical parameter T_{50G} , the temperature at which $2T'_{zz}$ equals 50G. Values of T_{50G} are obtained conveniently from plots of $2T'_{zz}$ versus temperature which are typically sigmoidal in form as in Fig. 4 (Ref. 12). For the polymers included in Fig. 4 there is an obvious correlation between the T_{50G} values and the glass transition

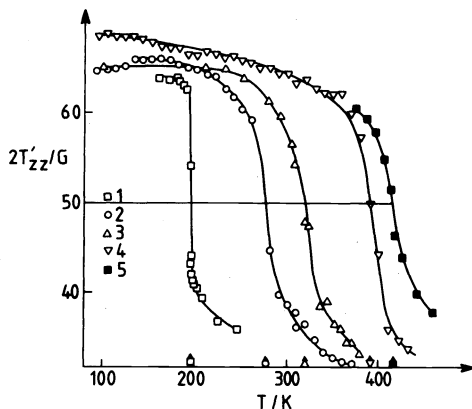


Fig. 4. Extrema separation ($2T'_{zz}$) versus temperature of the ESR spectra of probe 4 in poly(dimethylsiloxane) (1), high density polyethylene (2), polyisobutylene (3), poly(vinyl chloride) (4), and polycarbonate (5). T_{50G} values shown by arrows. (Reproduced with permission from Ref. 12).

temperatures, T_g . The sharp decrease in extrema separation reflects a marked increase in probe mobility which would be expected to occur with the onset of rapid motion in the macromolecules themselves, and hence a link between T_{50G} and T_g is not surprising. However, the plot of T_{50G} versus T_g in Fig. 5 (Ref. 13) shows that T_{50G} is generally $> T_g$. The effective frequency at T_{50G} is about 5×10^7 Hz, whilst the T_g values in Fig. 5 refer to frequencies of ~ 1 Hz. Thus, T_{50G} may be considered as a high-frequency glass transition temperature.

In principle an unknown T_g could be determined by measuring T_{50G} with probe 4 and reading off the corresponding T_g value from Fig. 5. It is unlikely, however, that the spin-probe method will become a routine or even a common route to T_g determinations, though there are two areas in which the technique has proved to have particular utility. The glass transition temperature of polyethylene has been a subject of controversy for some time. Kumler and Boyer (13) measured T_{50G} 's for probe 4 in a series of ethylene-propylene and ethylene-vinyl acetate copolymers and converted these to T_g 's by means of the calibration curve in Fig. 5. The ESR data lay close to the Gordon-Taylor extrapolation of earlier literature data obtained by conventional methods and indicated a T_g of ca. -80°C for pure polyethylene.

Other independently obtained data (Ref. 14 & 15) support a value of T_g in this region.

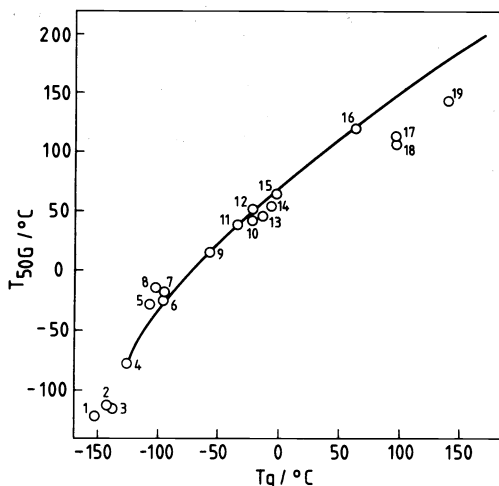


Fig. 5. T_{50G} versus T_g for various polymers with probe 4. Poly(dimethylsiloxane) (PDMS - 236) (1), PDMS - 384 (2), PDMS - 540 (3), PDMS (4), Budene (5), Diene 55 (6) and (7), polypentenamer (8), ethylene-propylene 50/50 copolymer (9), polypropylene (10), styrene-butadiene copolymer 42 wt. % styrene (S/B-42) (11), S/B-52 (12), S/B-57 (13), S/B-60 (14), S/B-62 (15), poly(vinyl chloride) (16), polystyrenes-705 and 706 (17) and (18), and polycarbonate (19). Data points from Table I of Ref. 13. Theoretical curve computed from eqn. 3 of Ref. 13 with data from Table II of Ref. 13.

The T_{50G} values in Fig. 5 were obtained with probe 4 and it is well established that the T_{50G} value for a particular polymer increases as the molecular volume of the probe increases. Therefore, before the ESR method can be employed to measure T_g 's the probe has to be carefully calibrated with polymers of known T_g . The variation in T_{50G} with probe volume has been studied in detail by Kusumoto (16) who derived the following relationship between T_g and T_{50G}

$$T_{50G} - T_g = 52[2.9f(\ln 1/f + 1) - 1] \quad (9)$$

where f is the ratio of the molecular volume of the probe to that of the polymer segment undergoing relaxation. Kusumoto showed that data from a range of probes, of varying molecular volume, in vulcanized natural rubber could be fitted to a common curve of T_{50G} versus f , corresponding to 45 backbone atoms in the relaxing rubber segment. Poly(vinyl acetate) (PVAc) containing probe 7 gave $f = 0.125$, (Ref. 17) indicating that the segment volume is approximately eight times that of the probe. With the bulkier probe 8 the value of f increases to 0.40 (Ref. 18).

The experiments with PVAc included measurements in the presence of plasticiser. The molecular volume and structure of the plasticiser dimethyl phthalate are quite similar to those of the probe 7, so that the effect of the probe on the physical properties of such systems is minimised. It was observed (Ref. 17 & 18) that T_{50G} 's of plasticiser-polymer compositions follow the relationship

$$\frac{1}{T_{50G}} = \frac{w_1}{T_{50G 1}} + \frac{w_2}{T_{50G 2}} \quad (10)$$

where w refers to mass, and the subscripts 1 and 2 to polymer and plasticiser respectively. Equation 10 is of course the well known relationship (Ref. 19) for the variation of T_g with composition; this is further evidence that T_{50G} is a high-frequency T_g . According to the literature, dinonyl phthalate is immiscible with PVAc and when this solvent, doped with the dinonyl probe 9, is mixed with approximately equal amounts of polymer the T_{50G} value is the same as that of spin-probed pure solvent. This indicates that the system comprises two phases - polymer and solvent - with the probe concentrated in the latter. Small amounts of dinonyl phthalate are compatible with PVAc and up to ca. 17% gives the same plasticising effect as the lower phthalate esters (Fig. 6). At > 17% plasticiser the ESR spectrum is a superposition of two spectra, and two T_{50G} values are obtained - the upper value corresponding to plasticised polymer and the lower to free plasticiser (Ref. 18).

Values of T_{50G} increase with increasing probe size and therefore a spin-labelled polymer, which can be viewed in terms of size and bulk as the ultimate spin probe, would be expected to have a much higher T_{50G} than the same polymer containing a small nitroxide probe. The

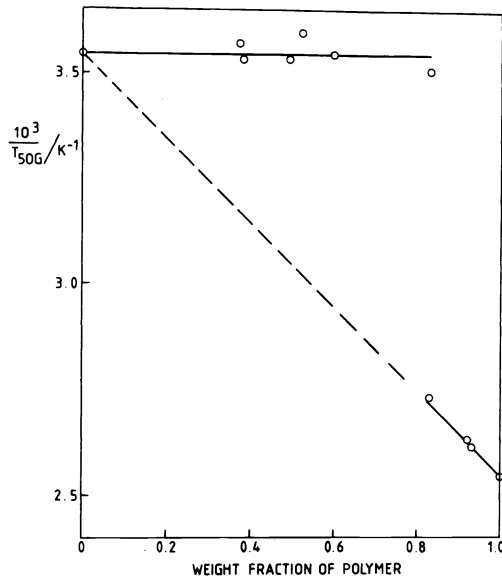


Fig. 6. T_{50G}^{-1} versus weight fraction of polymer for the system poly(vinyl acetate) - dinonyl phthalate with probe ρ .

gap between the T_{50G} values from probed and labelled polymers, however, is not as great as might be expected. This arises because the trend in T_{50G} with probe size eventually reaches a limit; ultimately the nitroxide moiety acquires a degree of motional independence over other parts of the probe molecule. Viewed in this way, there is no distinct division between spin probes and spin labels (Ref. 12). Interest in spin-labelled polymers has not centred round the T_{50G} parameter but rather on the information they can yield on the dynamics and energetics of polymer chains in bulk and in solution.

RELAXATIONS AND PHASE TRANSITIONS IN BULK POLYMERS

If correlation times for probe or label tumbling are plotted against reciprocal temperature in Arrhenius fashion then transitions are revealed as discontinuities. Typical plots of this sort as shown in Fig. 7 (Ref. 20) where the region of change in slope for each polymer lies close to T_g . At temperatures below T_g the correlation times are quite long and the activation energies for probe tumbling are low (4-11 kJ mol⁻¹). It has been postulated that below T_g probe motion is largely independent of macromolecular motions and is determined by the static free volume of the polymer. Above T_g probe motion is determined not only by the free volume but by dynamic fluctuations due to greatly increased macromolecular motions. The higher energy of activation for the latter is reflected in an increase in activation energy for probe tumbling above T_g .

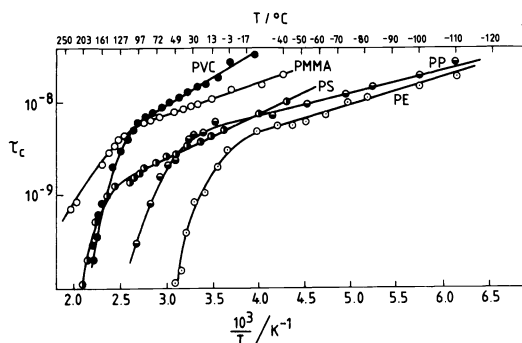


Fig. 7. Arrhenius plots of correlation times of probe 1 in various polymers. (Redrawn with permission from Ref. 12).

From Fig. 7 it is possible to estimate a temperature T_d for the discontinuity in the Arrhenius plot and it has been argued (Ref. 20) that a $T_d - T_g$ comparison is more valid than the $T_{50G} - T_g$ correlation, because the glass transition is not an isofrequency point for rotation of small molecules in polymers. There is some validity in this comment, but it is undeniable that T_{50G} is much more easily determined than T_d and, providing that the probe is calibrated carefully, experimental plots such as Fig. 5 should give fairly reliable high frequency T_g values.

Although the characteristics of probe tumbling are intimately affected by the dynamic state of the host polymer, particularly above T_g , the frequency and energetics of motion of the probe are not necessarily equal to those of the host. This statement underlines one of the weaknesses of the spin-probe experiment. It also provides a striking contrast to the information afforded by spin-label studies of polymers in solution where, in favourable cases, the dynamic characteristics of the label can be identified with those of the polymer chain segment (Ref. 5). A similar situation prevails with spin-labelled polymers in the solid and molten phases. There are not too many cases in which the polymer melt is accessible to spin-label or probe studies because the lifetime of many nitroxides is rather short at the relatively high temperatures required. Polyethylene, however, provides an interesting example of the potential of the spin-label method for bulk phase studies (Ref. 3).

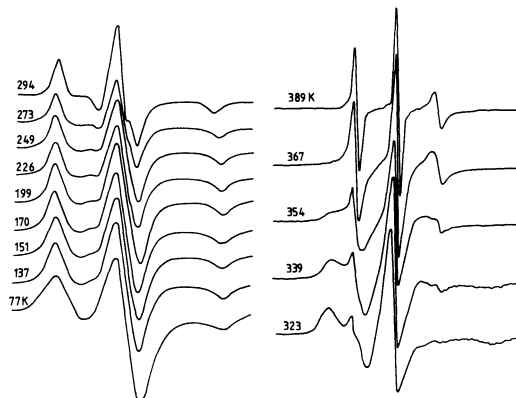


Fig. 8. ESR spectra of bulk low density polyethylene PE/CO labelled as in 11. (Taken with permission from Ref. 3).

The ESR spectra of low density polyethylene PE/CO labelled with the oxazolidine nitroxide 11 were recorded over the temperature range 77 - 390K. From the representative spectra in Fig. 8 it can be seen that the motion of the radical label varies from near the rigid limit to the fast region over this temperature range. Correlation times, calculated by the appropriate techniques described above, are shown as an Arrhenius plot in Fig. 9. Two well-defined transition temperatures are apparent; the upper temperature corresponds to the melting point T_m . In the temperature region below the lower transition temperature 350K, it seems likely that the β -relaxation is being observed. The activation energy for motion in this region lies in the range 29 kJ mol⁻¹ for "amorphous" polymer to 24 kJ mol⁻¹ for the annealed sample. (The shorter correlation times and lower energy of activation on annealing probably result from the reformation of crystalline regions from which irregularities or impurities are excluded. Annealing therefore places the label in the more amorphous regions of the sample where motion is less restricted.) These figures are in reasonable agreement with the values 24 - 33 kJ mol⁻¹ obtained from proton NMR relaxation studies over a similar temperature range. The discontinuity in the correlation map at 350K corresponds to T_α , and between T_α and T_m the α -relaxation is being observed. Unfortunately the correlation times at temperatures below 225K were too long to be calculated from measurements of extrema separations and hence it was not possible to observe the β -transition temperature or derive a value of T_g .

The correlation map in Fig. 9 includes data for the labelled PE/CO polymer in xylene solution and it is instructive to compare these with the data from the molten polymer. The activation energy for relaxation in solution is 22.9 \pm 1.9 kJ mol⁻¹ and since the nitroxide label in this polymer cannot move independently of the carbon backbone this energy barrier must be associated with that of chain motion. Also, since the molecular weight of this polymer was ca. 100,000, relaxation in solution can be attributed to local segmental modes with a negligible contribution from whole-molecule rotation. Therefore, the activation energy for rotation in the "isolated" polymer molecule can be obtained by subtracting from this figure 9.0 \pm 0.3 kJ mol⁻¹ for the activation energy of viscous flow of xylene. This yields ca. 14 \pm 2 kJ mol⁻¹ as the energy barrier to internal rotations in the polymer, a figure which is remarkably close to the 12 kJ mol⁻¹ barrier to internal rotations in ethane molecules in the gas phase (Ref. 21). In the molten state, where whole-molecule tumbling is also insignificant, the overall activation energy for relaxation is 15.2 \pm 1.5 kJ mol⁻¹. But the energy of activation for viscous flow of molten polyethylene is 46 - 61 kJ mol⁻¹ (Ref. 22) and clearly viscous drag of the type exerted by solvent on polymer segments does not operate in the bulk, molten polymer. In other words, the energy barrier to segmental rotation in the molten polymer is not much greater than the internal barriers to rotation in an isolated polymer chain. This is in general accord with Bueche's hypothesis (Ref. 23) that in the melt, chain segments are surrounded by equivalent segments and there is no hydrodynamic shielding. Thus, the reason why relaxations in the melt are slower than in solution is not because the energy barriers are greater in the melt but because the pre-

exponential factor for rotations in the melt ($1.5 \times 10^{10} \text{ s}^{-1}$) is lower than in the isolated molecule ($9.5 \times 10^{10} \text{ s}^{-1}$).

Polyethylene containing a small proportion of copolymerised methyl vinyl ketone (PE/MVK) has also been labelled by the Keana method to yield labelled units 13 (Ref. 3).

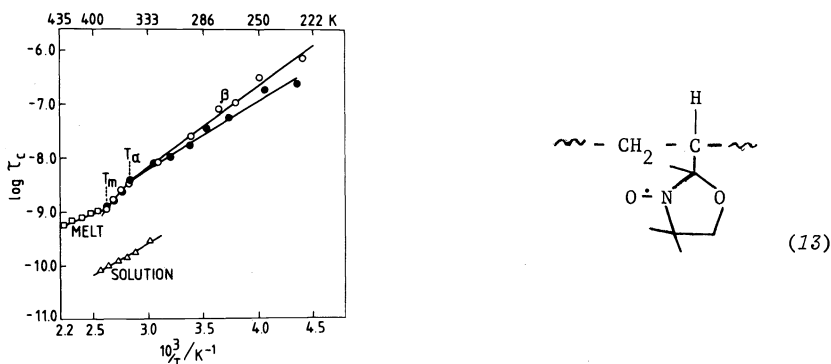


Fig. 9. Arrhenius plot of τ_c for spin-labelled low density polyethylene. (Taken with permission from Ref. 3).

Unlike 11 this structure is pendent to the main chain and has a degree of mobility independent of segmental motion. As a result, the correlation times for labelled PE/MVK in solution are about half of those for labelled PE/CO under the same conditions, and the energy barriers to rotation in bulk labelled PE/MVK are lower than in bulk PE/CO. This observation underlines the need for care in interpreting data from ESR studies of spin-labelled polymers. In the absence of adequate supporting evidence it is unwise to assume that the motion of the label replicates exactly that of the main polymer chain. Indeed, it has been demonstrated that if the spin-label is separated from the polymer chain by a sufficiently long flexible chain the correlation time can decrease to a value characteristic of the free nitroxide (Ref. 24).

REFERENCES

1. T.J. Stone, T. Buckman, P.L. Nordio and H.M. McConnell, *Proc. Natl. Acad. Sci. U.S.A.*, **54**, 1010 (1965).
2. J.F.W. Keana, S.B. Keana and J. Beetham, *J. Am. Chem. Soc.*, **89**, 3055 (1967).
3. A.T. Bullock, G.G. Cameron and P.M. Smith, *Eur. Polym. J.*, **11**, 617 (1975); A.T. Bullock, G.G. Cameron and P.M. Smith, *Macromolecules*, **9**, 650 (1976).
4. A.T. Bullock, G.G. Cameron and N.K. Reddy, *J. Chem. Soc., Faraday I*, **74**, 727 (1978).
5. A.T. Bullock, G.G. Cameron and P.M. Smith, *J. Phys. Chem.*, **77**, 1635 (1973).
6. R.C. McCalley, E.J. Shimshick and H.M. McConnell, *Chem. Phys. Lett.*, **13**, 115 (1972).
7. S.A. Goldman, G.V. Bruno and J.H. Freed, *J. Phys. Chem.*, **76**, 1858 (1972).
8. R. Mason and J.H. Freed, *J. Phys. Chem.*, **78**, 1321 (1974).
9. A.N. Kuznetsov and B. Ebert, *Chem. Phys. Lett.*, **25**, 342 (1974).
10. J.H. Freed in *Spin Labelling. Theory and Applications*, p.53, L.J. Berliner, Ed., Academic Press, New York, 1974.
11. A. Hudson and G.R. Luckhurst, *Chem. Rev.*, **69**, 191 (1969).
12. P. Törmälä, in *Molecular Motion in Polymers by ESR*, p.88, R.F. Boyer and S.E. Keinath, Ed., Harwood, Chur, 1980.
13. P.L. Kumler and R.F. Boyer, *Macromolecules*, **9**, 903 (1976).
14. J.M.G. Cowie and I. McEwan, *Macromolecules*, **10**, 1124 (1977).
15. G.G. Cameron in Ref. 12, p. 55; A.T. Bullock, G.G. Cameron and N.K. Reddy, unpublished results; B. Florin, R. Spitz, A. Douillard, A. Guyot, R.F. Boyer, D.L. Richards and P.L. Kumler, *Eur. Polym. J.*, **16**, 1079 (1980).
16. N. Kusumoto, S. Sano, N. Zaitso and Y. Motozato, *Polymer*, **17**, 448 (1976); N. Kusumoto in Ref. 12, p. 223.
17. A.T. Bullock, G.G. Cameron, C.B. Howard and N.K. Reddy, *Polymer*, **19**, 352 (1978).
18. A.T. Bullock, G.G. Cameron and I.S. Miles, to be published in full.
19. L. Mandelkern, G.M. Martin and F.A. Quinn, *J. Res. Nat. Bur. Stand. U.S.A.*, **58**, 177 (1959).
20. A.L. Kovarskii, J. Plaček and F. Szöcs, *Polymer*, **19**, 1137 (1978).
21. E.B. Wilson, *Adv. Chem. Phys.*, **2**, 367 (1959).
22. H. Schott and W.S. Kaghani, *J. Appl. Polym. Sci.*, **5**, 175 (1961).
23. F. Bueche, *Physical Properties of Polymers*, Interscience, New York, 1962.
24. J. Labský, J. Pilař and J. Kálal, *Macromolecules*, **10**, 1153 (1977); J. Pilař, J. Labský, J. Kálal and J.H. Freed, *J. Phys. Chem.*, **83**, 1907 (1979).